Journal of Integrative Agriculture 2026, 25(7): 2959–2969

Available online at ScienceDirect

Journal of Integrative Agriculture



RESEARCH ARTICLE

Collateral sensitivity to gamithromycin in ciprofloxacin-resistant *Streptococcus suis* is driven by increasing intracellular antibiotic accumulation

Yuejun Zhang[1, 2], Mengting Tao[3], Ruiling Wang[1, 2], Zilin Shi[1, 2], Peipei Li[1, 2], Sijia Tang[1, 2], Jian Sun[1, 2, 4], Xiaoping Liao[1, 2, 4], Yufeng Zhou[1, 2, 4#]

[1] *State Key Laboratory of Animal Disease Control and Prevention, College of Veterinary Medicine, South China Agricultural University, Guangzhou 510642, China*

[2] *Guangdong Provincial Key Laboratory of Veterinary Pharmaceutics Development and Safety Evaluation, South China Agricultural University, Guangzhou 510642, China*

[3] *Institute of Laboratory Animal Science, Jinan University, Guangzhou 510632, China*

[4] *Jiangsu Co-Innovation Center for the Prevention and Control of Important Animal Infectious Disease and Zoonosis, Yangzhou University, Yangzhou 225009, China*

Highlights

- A complex network of collateral sensitivity was characterized in *Streptococcus suis*.
- Gamithromycin exhibited collateral sensitivity toward ciprofloxacin-resistant *S. suis*.
- Altered membrane potential and reduced efflux pump activity lead to increased intracellular antibiotic levels.
- Elevated intracellular accumulation of gamithromycin contributes to collateral sensitivity in ciprofloxacin-resistant *S. suis*.

Abstract

Streptococcus suis has garnered increasing attention due to its implication in severe infections in both swine and humans, as well as its development of multidrug resistance. The phenomenon of collateral sensitivity, whereby resistance to one antibiotic leads to increased sensitivity to another, provides new opportunities for mitigating the evolution of resistance. In this study, we evolved resistance in *S. suis* to 11 clinically used antibiotics and characterized the resulting collateral sensitivity profiles, revealing a complex network of interactions. Based on our findings, we identified dozens of such drug pairs and demonstrated collateral sensitivity to gamithromycin in ciprofloxacin-resistant *S. suis* both *in vitro* and *in vivo*. Gamithromycin effectively limits the evolution of resistance and reduces the mutant selection window for ciprofloxacin-resistant *S. suis* strains. Mechanistic studies indicated that the heightened sensitivity of ciprofloxacin-resistant *S. suis* to gamithromycin was associated with increased intracellular gamithromycin accumulation due to membrane potential alterations and reduced functions of proton motive force (PMF)-dependent efflux pumps. Furthermore, collateral sensitivity-based treatments significantly resensitized ciprofloxacin-resistant *S. suis* strains to gamithromycin, resulting in superior efficacy, lower pharmacodynamic targets, and higher treatment success rates in a murine thigh infection model. Our results indicate that gamithromycin sensitivity in *S. suis* is a collateral consequence of resistance to ciprofloxacin, providing valuable insight for the strategic design of collateral sensitivity-based antibiotic therapies for *S. suis* infections.

Keywords: collateral sensitivity, *S. suis*, gamithromycin, ciprofloxacin

1. Introduction

Streptococcus suis is a significant zoonotic pathogen capable of causing systemic diseases in both pigs and humans, posing a threat to global public health (Segura 2009; Dong *et al.* 2021). Clinical manifestations of *S. suis* infections include bacteremia, meningitis, endocarditis, and streptococcal toxic shock syndrome (Tang *et al.* 2006; Pan *et al.* 2022; Mei *et al.* 2025). Among the 29 known serotypes, *S. suis* serotype 2 (SS2, a highly virulent type) is widely recognized as the most prevalent, accounting for 43.2% of clinical isolates in humans

Received 1 June 2024; Received in revised form 25 September 2024; Accepted 22 October 2024; Available online 5 December 2024
#Correspondence Yufeng Zhou, Tel/Fax: +86-20-85288387, E-mail: zyf@scau.edu.cn

© 2026 CAAS. Publishing services by Elsevier B.V. on behalf of KeAi Communications Co. Ltd. This is an open access article under the CC BY-NC-ND license (http://creativecommons.org/licenses/by-nc-nd/4.0/). Peer review under responsibility of Editorial Board of *Journal of Integrative Agriculture*.
doi: 10.1016/j.jia.2024.12.005

and pigs (Feng *et al.* 2010, 2014; Shi *et al*. 2024). Consistent with these findings, our recent investigation revealed that SS2 constituted 41.7% (40/96) of *S. suis* isolates collected in China from 2008 to 2019 (Wang *et al*. 2023). Close occupational contact with pigs and pork products is often the primary cause of human *S. suis* infection. Over the past few decades, reported cases of *S. suis* infections in humans have significantly increased. Notably, two large-scale epidemics of severe SS2 infections occurred in China in 1998 and 2005, resulting in 240 human cases and 53 deaths (Tang *et al.* 2006; Yu *et al.* 2006; Zheng *et al.* 2020). Despite the availability of vaccinations against streptococcosis, antibiotics such as β-lactams, fluoroquinolones, and macrolides remain the primary treatments for *S. suis* infections due to the diversity of serotypes (Segura 2015; Haenni *et al.* 2018). However, the recent emergence of penicillin-resistant and multidrug-resistant strains has seriously limited treatment options for severe *S. suis* infections (Qu *et al.* 2023). Thus, novel therapeutic strategies are urgently needed to combat these resistant pathogens.

The trade-offs associated with antibiotic resistance are gaining attention for designing antibiotic dosing strategies that mitigate the emergence of resistance within the host (Aulin *et al.* 2021). Collateral sensitivity, whereby resistance to one antibiotic is accompanied by increased sensitivity to another, offers promising avenues for innovative therapeutic interventions against infections unresponsive to classical treatments (Roemhild and Andersson 2021). Previous studies have demonstrated collateral sensitivity phenotypes in various clinically relevant bacteria, including *Streptococcus pneumoniae*, *Staphylococcus aureus*, *Escherichia coli*, and *Pseudomonas aeruginosa* (Gonzales *et al.* 2015; Hernando-Amado *et al.* 2020; Roemhild *et al.* 2020; Liakopoulos *et al.* 2022). Among these bacteria, collateral sensitivity is a common pleiotropic consequence of resistance mutations, primarily observed between antibiotics with distinct killing mechanisms (Lázár *et al.* 2013; Roemhild *et al.* 2020). Thus, sequential multidrug treatments using antibiotics with collateral sensitivity may help mitigate the rate of resistance evolution, as supported by a growing body of experimental studies across various bacterial species (Fuentes-Hernandez *et al.* 2015; Yoshida *et al.* 2017). However, our understanding of the underlying mechanisms of collateral sensitivity remains limited.

In the present study, we characterize the collateral sensitivity profiles of antibiotic-resistant *S. suis* strains, focusing on the clinically significant SS2 representative strain, ATCC 43765. Our analysis identifies several non-synonymous mutations associated with increased sensitivity to gamithromycin (GAM) in ciprofloxacin (CIP)-resistant *S. suis* subpopulations. This collateral sensitivity in CIP-resistant *S. suis* mutants is partly attributed to regulatory mechanisms that increase intracellular antibiotic accumulation. These findings support the potential for sequential therapy combining macrolides and fluoroquinolones to enhance antibiotic activity against multidrug-resistant *S. suis* and to mitigate the evolution of antibiotic resistance.

2. Materials and methods

2.1. Media, bacterial strains and antibiotics

All antibiotic-resistant *S. suis* strains used in this study were derived from ATCC 43765. These strains were adapted to the 11 antibiotics listed in Appendix A. Antibiotic solutions were prepared from powder stock (Yuanye Biotechnology, Shanghai, China) and filter-sterilized. Gamithromycin injection (Zactran, 15%, w/v) for *in vivo* experiments was purchased from Boehringer Ingelheim Animal Health (Lyon, France). *S. suis* strains were grown, subcultured, and quantified using cation-adjusted Mueller-Hinton broth (CAMHB) supplemented with 5% lysed horse blood and on sheep blood agar (SBA; Difco Laboratories, Detroit, MI, USA).

2.2. *Streptococcus suis* strain adaptation and whole genome sequencing (WGS)

Streptococcus suis strains developed resistance to selected antibiotics by a gradient plate method on sheep blood agar (Szybalski and Bryson 1952). Briefly, log-phase *S. suis* colonies were streaked onto gradient plates and incubated overnight at 37°C. After incubation, the growth edge of the *S. suis* colonies was swept and reseeded onto a fresh gradient plate. This procedure was repeated until bacterial growth was observed across the entire plate, resulting in the evolution of laboratory-derived resistant *S. suis* strains. All evolved drug-resistant mutants were serially passaged by streaking onto SBA plates to assess phenotypic stability. After 10 consecutive days of passaging, the final evolved strains, including the CIP^R mutant and its parental strain, underwent susceptibility testing and WGS. Genomic DNA was extracted using a Bacterial Genome DNA Extraction Kit (Tiangen, Beijing), and WGS was performed on the Illumina HiSeq 2500 System (Novogene, Guangzhou, China).

2.3. Minimum inhibitory concentration (MIC), mutant prevention concentration (MPC) determinations, and susceptibility profiles

The MICs of 11 selected antibiotics for the wild-type (WT) *S. suis* ATCC 43765 and its evolved resistant mutants were determined using the microbroth dilution method in accordance with the Clinical and Laboratory Standards Institute (CLSI) guidelines (CLSI 2020). For the GAM^R and CIP^R *S. suis* mutants, the MPCs were determined by plating initial inocula of $10^{9.5}$ cfu mL^{-1} from overnight culture onto SBA plates supplemented with various concentrations of GAM or CIP (1×, 2×, 4×, 8×, 16×, 32×, 64×, and 128×MIC_{WT}). Viable bacterial growth was counted after overnight incubation at 37°C.

A strain susceptibility profile was generated based on the $\log_2$fold change in MICs between the WT and resistant mutants to visualize the collateral sensitivity network for *S. suis* ATCC 43765. Collateral sensitivity was defined as the inhibition of growth in resistant mutants at lower MICs compared to the WT.

2.4. *In vitro* time-growth and time-kill assays

Growth curves were established to compare the *in vitro* fitness of WT and resistant *S. suis* strains. Time-growth studies for all strains were performed by inoculating CAMHB

with an overnight culture (1:100 dilution) and incubating at 37°C overnight. The optical density (OD) at 600 nm was monitored hourly over a 24 h period.

Time-kill experiments were performed to assess the *in vitro* activity of GAM and CIP against the WT and resistant strains. An initial inoculum of approximately 5×10^5 cfu mL^{-1} *S. suis* cells from an overnight culture was inoculated into MHB supplemented with GAM or CIP at 16×MIC. After 3, 6, 9, and 12 h of incubation, serial dilutions were plated onto blood agar for bacterial enumeration. In addition, each *S. suis* strain at approximately 1×10^6 cfu mL^{-1} was incubated in 10 mL of CAMHB supplemented with various concentrations of GAM (0.004–0.25 mg L^{-1}) or CIP (0.25–16 mg L^{-1}). After 18 h of incubation, serial dilutions were plated onto blood agar for colony counts. Strain survival was calculated as the final bacterial count after 18 h of exposure to GAM or CIP divided by the initial inoculum.

2.5. Construction of Δ*ktrB S. suis* strain

The *ktrB* gene-inactivated *S. suis* ATCC 43765 mutant (designated as Δ*ktrB*; Appendix B) was generated *via* allelic replacement with a spectinomycin resistance (SPC^R) cassette using a previously described method (Cao *et al.* 2011). The upstream and downstream DNA fragments flanking *ktrB* were amplified and cloned into the pUC19 vector using the ClonExpress II One Step Cloning Kit (Vazyme Biotech Co., China). The resulting vector was inserted with the SPC^R gene (derived from the *E. coli-S. suis* shuttle vector pSET2) to create the *ktrB* knockout plasmid, designated as pUC19::*ktrB* (Appendix B). This knockout plasmid was electroporated into the WT using an electroporation system (voltage, 2300 V; capacitance, 25 μF; resistance, 200 Ω; cuvette, 1 mm). Transformants resistant to SPC were initially screened by PCR, and suspected mutants were further confirmed using Sanger sequencing and WGS.

2.6. Construction of the *pmrA*-overexpression *S. suis* strain

The open reading frame of the *pmrA* gene, including its upstream promoter and downstream sequence, was amplified from the chromosomal DNA of the WT strain and cloned into the pSET2 vector to create the plasmid pSET2-*pmrA* (Appendix B). The resulting plasmid was then electroporated into the WT strain to generate the *pmrA*-overexpression *S. suis* strain, designated as WT(*pmrA*).

2.7. Plasma membrane permeability assay

Fluorescent probe 1-N-phenylnaphthylamine (NPN) was used to evaluate the plasma membrane permeability of WT and drug-resistant mutants (Wang *et al.* 2022). Fluorescence intensity was measured with an excitation wavelength of 355 nm and an emission wavelength of 405 nm (Zhao *et al.* 2023).

2.8. Cell membrane integrity assay

The integrity of the cell membrane in WT and drug-resistant mutants was measured using the fluorescence intensity of propidium iodide (PI), with an excitation wavelength of 535 nm and an emission wavelength of 615 nm (Weng *et al.* 2023).

2.9. Membrane depolarization

The membrane potential of the WT, CIP^R, and Δ*ktrB* strains was measured using 3,3′-dipropylthiocarbocyanine iodide [$DiSC_3(5)$; 0.5 μmol L^{-1}]. Dissipated bacterial membrane potential was determined with an excitation wavelength of 622 nm and an emission wavelength of 670 nm (Lee *et al.* 2015).

2.10. Proton motive force (PMF) assay

The PMF of the WT, CIP^R, and Δ*ktrB* strains in the presence or absence of carbonyl cyanide m-chlorophenylhydrazone (CCCP; 5 μmol L^{-1}) was measured with the fluorescence probe bis-carboxyethyl-carboxyfluorescein acetoxymethyl ester (BCECF-AM). The fluorescence intensity of BCECF-AM-stained *S. suis* cells was recorded with an excitation wavelength of 485 nm and an emission wavelength of 535 nm (Yang *et al.* 2023).

2.11. Intracellular adenosine triphosphate (ATP) measurement

Intracellular ATP levels of the WT, CIP^R, and Δ*ktrB* strains with or without CCCP treatment were determined using a Luciferase ATP Assay Kit (Beyotime, Shanghai, China) as previously described (Li *et al.* 2022). Briefly, each strain at about 10^8 cfu mL^{-1} was lysed with lysozyme and sonication. The lysate supernatant was collected and mixed with detection solution containing luciferase in a 96-well plate. Luminescence was measured using an EnSight multimode plate reader (PerkinElmer, USA), and ATP levels were calculated based on a calibration curve derived from standard ATP samples.

2.12. Quantitative real-time PCR (qRT-PCR) analysis

The qRT-PCR was used to detect the mRNA expression levels of *pmrA* and *ktrB* relative to the control gene (16S rRNA) in WT and CIP^R strains (Dou *et al.* 2023). Total RNA was extracted from cultured bacterial cells after 24 h at 37°C using a Bacterial RNA Extraction Kit (Omega Bio-Tek, USA). Purified RNA was further reverse-ranscribed into cDNA and amplified with SYBR Green PCR Master Mix (TaKaRa, Japan). Relative quantification was calculated using the threshold cycle ($2^{-\Delta\Delta CT}$) method.

2.13. Intracellular GAM accumulation

The intracellular GAM accumulations in the WT, CIP^R, and WT (*pmrA*) strains, with or without CCCP and phenyl-arginine-β-naphthylamide (PaβN; 50 μmol L^{-1}; Sigma-Aldrich, Germany), were determined as previously reported (Wang *et al.* 2022). *Streptococcus suis* cells from an overnight culture were adjusted to approximately 10^{10} cfu mL^{-1} and incubated with GAM at 2 mg L^{-1} for 15 min. After centrifugation, precipitated bacteria were washed three times with phosphate buffered saline (PBS) and lysed by sonication (200 W total power, 35% output, 2 s pulse, 3 s pause on ice) for 10 min (Chen *et al.* 2023). GAM concentrations in the lysate were determined by liquid chromatography-tandem mass spectrometry (LC-MS/MS) as previously described (Zhou *et al.* 2020), with a limit of quantification (LOQ) of 0.001 mg L^{-1}.

2.14. GAM pharmacokinetic (PK) analysis

Specific-pathogen-free ICR mice (6 weeks old, 25–30 g) were purchased from the Guangdong Medical Lab Animal Center (Guangzhou, China). Plasma pharmacokinetics (PKs) of GAM in mice were determined after subcutaneous (s.c.) administrations of 3, 6, and 12 mg kg^{-1}. Groups of six mice were sampled at various time points (0.25, 0.5, 0.75, 1, 3, 6, 9, 12, 36, 48, and 60 h) and dose levels. Blood samples were obtained by retro-orbital puncture at the specified time points. Plasma was isolated by centrifugation at 3,000×g for 10 min. GAM concentrations in plasma were quantified using an LC-MS/MS method as described previously (Zhou *et al.* 2020; Wei *et al.* 2024). Multiple reaction monitoring transitions selected in positive mode were m/z [$(M+2H)^{2+}$] 389.7→83.1 and 389.7→115.2 for GAM. The limit of quantification (LOQ) and limit of detection (LOD) were 0.001 and 0.0005 mg L^{-1}, respectively. Average recoveries of GAM in plasma were >90%, and relative standard deviations (RSDs) for both interday and intraday were <10%. All PK parameters were calculated using a non-compartmental model in Phoenix WinNonlin software (version 8.4, Certara, NJ, USA).

2.15. Murine thigh infection model

Mice were rendered neutropenic by administration of cyclophosphamide intraperitoneally 4 days (150 mg kg^{-1}) and 1 day (100 mg kg^{-1}) before infection. Thigh infections with WT and CIP^R *S. suis* strains were established by injecting 100 µL of an early log-phase bacterial suspension (10^6 cfu mL^{-1}) into the thigh. At 2 h after infection, mice were randomized to receive: (i) control treatment with the vehicle, (ii) GAM at 24 mg kg^{-1} s.c. once daily. This dose was chosen to simulate the PK profile achieved by the recommended intramuscular dose of 6 mg kg^{-1} in piglets (Zhou *et al.* 2020). Treatment lasted for 24 h, after which mice were euthanized, and thigh tissues were aseptically harvested, homogenized, and quantitatively cultured to determine the mean $\log_{10}$ cfu g^{-1} tissue (±SD; *n*=5 to 7). In addition, the strains recovered from thigh tissues post-treatment were isolated to evaluate phenotypic and genotypic stability of collateral sensitivity.

2.16. *In vivo* pharmacodynamic (PD) target comparison

In vivo treatment studies were performed using the murine thigh infection model with WT and CIP^R strains as described above. Five total dose regimens of GAM, ranging from 2.5 to 24 mg kg^{-1} every 24 h, were selected to identify the entire dose-response relationship from maximum to no efficacy. After 24 h of treatment, bacterial burdens were enumerated from thigh homogenates.

The area under the concentration-time curve (AUC)/MIC ratio was chosen as the predictive PK/PD index to describe GAM efficacy (Toutain *et al.* 2021). The correlation between AUC/MIC and efficacy was determined by the sigmoid E_{max} model: $E=(E_{max}\times C^N)/(EC_{50}{}^N+C^N)$, where E is the effector (the pre-post treatment change in $\log_{10}$cfu g^{-1} per thigh), C is the AUC/MIC ratio being examined as well as the 24 h total dose, EC_{50} is the AUC/MIC ratio achieving 50% of the maximum effect (E_{max}), and N is the Hill coefficient. The AUC/MIC targets for the 1-$\log_{10}$ and 2-$\log_{10}$ kill effects were compared between WT and CIP^R strains.

2.17. GAM dose assessment between WT and resistant strains

Given the characteristics of collateral sensitivity to GAM in CIP^R *S. suis*, a 10,000-subject Monte Carlo simulation (Crystal Ball software, version 11.1, Oracle Corporation, California, USA) was performed to compare the probability of target attainment (PTA) for the current clinical dose of GAM (6 mg kg^{-1}) between WT and CIP^R strains. In addition, the optimum dose regimens of GAM necessary to achieve a bactericidal effect against WT and CIP^R strains were calculated by the following equation: $Dose=(Cl\times AUC/MIC_{breakpoint}\times MIC_{WT/R})/(fu\times F)$, where Cl is body clearance, $AUC/MIC_{breakpoint}$ is the *in vivo* target value required for a bactericidal effect. In this study, the AUC/MIC ratios were 86.7 h and 49.9 h for WT and CIP^R strains, respectively. The free drug fraction (*fu*) is 77%, using a binding rate of 23% (Wyns *et al.* 2014). The bioavailability (F) is 87.2% for the s.c. route (Zhou *et al.* 2020). Given that GAM is an animal-specific antibiotic approved for use in pigs, the PK parameters (Cl, *fu*, and F) used for dose assessments were derived from our previously published data in pigs (Zhou *et al.* 2020).

3. Results

3.1. Collateral sensitivity and cross-resistance patterns of antibiotic-resistant *S. suis* strains

The WT *S. suis* strain ATCC 43765 was exposed to 11 clinically relevant antibiotics to obtain the parallel-evolved bacterial lineages. The MICs for the 11 drug-resistant *S. suis* strains during adaptation in broth were consistently higher than the current CLSI or European Committee on Antimicrobial Susceptibility Testing (EUCAST) Clinical Breakpoints (Appendix A). For each drug-resistant isolate, changes in MICs were determined to exhibit collateral sensitivity and cross-resistance profiles for the 11 antibiotics. With the exception of the tetracycline-resistant isolate, all drug-resistant *S. suis* isolates demonstrated collateral sensitivity to at least two other antibiotics (Fig. 1-A and B). Of note, certain antibiotics such as gentamicin, cefotaxime, CIP, and GAM were more frequently included in the identified collateral sensitivity cycles (Fig. 1-C). In particular, a strong reciprocal collateral sensitivity cycle was noted between CIP and GAM (Fig. 1-D and E). This collateral sensitivity remained stable following 10 days of *in vitro* passaging and subsequent *in vivo* antibiotic treatment. Furthermore, we observed a general pattern of cross-resistance among antibiotics belonging to the same drug class or sharing similar antibacterial mechanisms (Fig. 1-A). Significant cross-resistance was observed, with a >4-fold increase in MIC between CIP and levofloxacin, GAM and erythromycin, as well as tetracycline and erythromycin (Fig. 1-A, D and E). Given the frequent use and critical importance of macrolides and tetracyclines in both human and veterinary medicine, clinicians should remain vigilant regarding potential treatment failure of *S. suis* infections due to their cross-resistance.

3.2. Impact of collateral sensitivity on growth and bactericidal kinetics

To assess whether collateral sensitivity cycling incurs adaptive

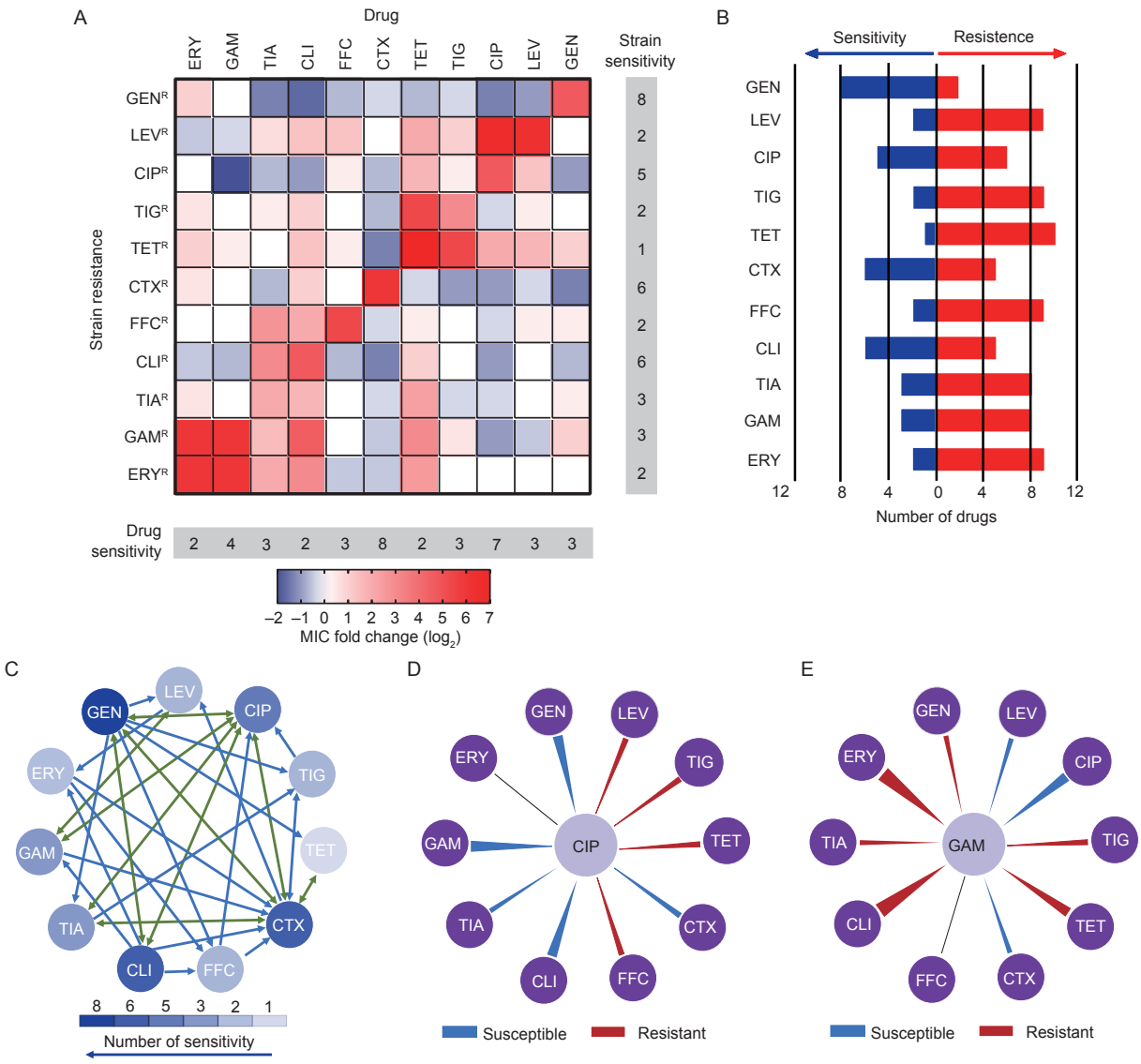


Fig. 1 Collateral sensitivity and cross-resistance profiles of antibiotic-resistant *Streptococcus suis* strains. A, a heat map illustrating the susceptibility profiles of antibiotic-resistant *S. suis* strains in comparison to the wild-type (WT) strain. Susceptibility profiles of *S. suis* were defined based on the minimum inhibitory concentration (MIC) changes with respect to the WT. B, distribution of collateral sensitivity and cross-resistance for 11 antibiotic-resistant *S. suis* mutants. In panels A and B, blue coloring refers to collateral sensitivity, red coloring refers to cross-resistance, and white coloring refers to no change in MIC relative to the WT. C, antibiotic pairs with collateral sensitivity. The nodes are color-coded in blue to represent the number of antibiotics with collateral sensitivity. A green double-headed arrow refers to reciprocal collateral sensitivity between antibiotic pairs, while a blue single-headed arrow refers to a one-directional collateral sensitivity relationship. D and E, diagrams illustrating the degree of convergence of collateral sensitivity and cross-resistance in ciprofloxacin (CIP)-resistant (D) and gamithromycin (GAM)-resistant (E) *S. suis* subpopulations derived from ATCC 43765. Drug abbreviations are shown in Appendix A.

costs, we monitored the growth kinetics of the WT, CIP^R, and GAM^R strains using spectrophotometry. The growth curve of the GAM^R strain was similar to that of the WT during the early log phase but exhibited a decline during the stationary phase (Fig. 2-A). In contrast, the growth curve of the CIP^R strain remained significantly lower than that of the WT throughout the observation period (Fig. 2-A), indicating an evolutionary trade-off associated with the acquisition of CIP resistance.

Exposure to GAM at 16×MIC$_{WT}$ preferentially killed the CIP^R *S. suis* cells (Fig. 2-B). Although the killing kinetics were similar, CIP at 16×MIC$_{WT}$ induced more rapid and complete bactericidal effects against the GAM^R cells compared to the WT strain (Fig. 2-C). In addition, selective elimination of resistant *S. suis* strains was observed based on collateral sensitivity cycling. Following GAM exposure, we found that CIP^R strains could be substantially cleared at GAM concentrations as low as 0.03 mg L^{-1} (Fig. 2-D). Similarly, CIP concentrations of >4 mg L^{-1} effectively cleared the GAM^R subpopulations (Fig. 2-E).

The MPC is defined as the concentration threshold above which no single-step drug-resistant mutant strains can be selected (Gianvecchio *et al.* 2019). Once the drug concentration at the site of infection exceeds the MPC, the emergence of resistance is expected to be limited. Our results

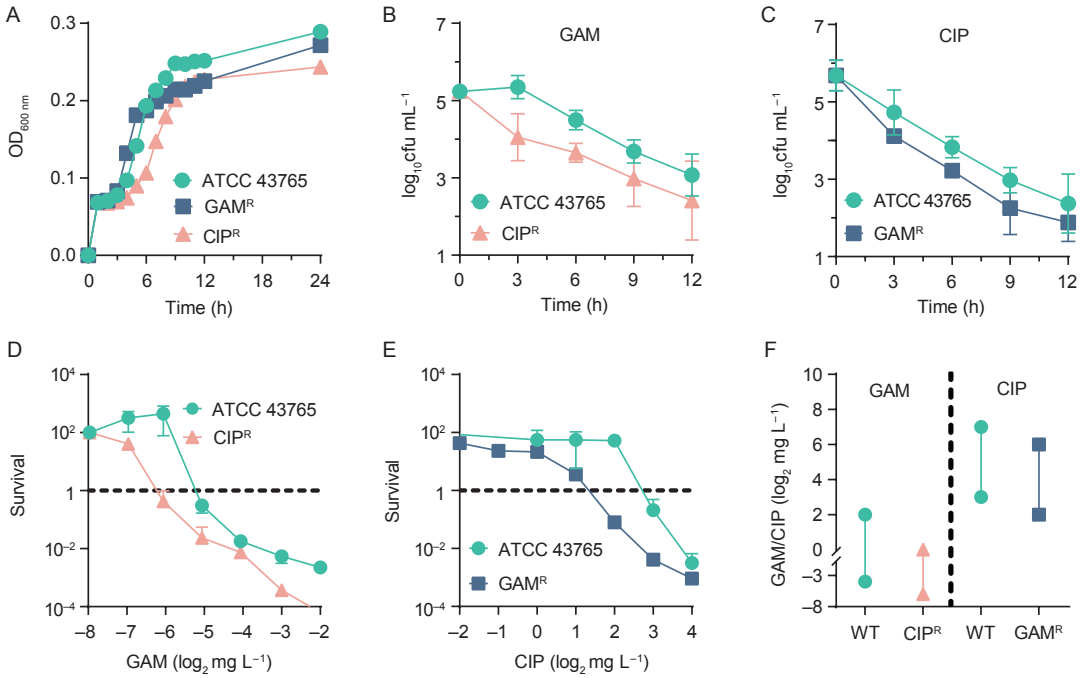


Fig. 2 Alteration of growth and killing dynamics, and mutant selection window of resistant *Streptococcus suis* strains by collateral sensitivity cycling. A–C, growth curve (A), time-kill curves of gamithromycin (GAM; B) and ciprofloxacin (CIP; C) against the wild-type (WT) *S. suis* ATCC 43765 strain and its resistant mutants. D and E, survival of the WT strain and its mutants resistant to gamithromycin (GAM^R) or ciprofloxacin (CIP^R) at various concentrations of GAM (D) and CIP (E). The dotted line represents the initial inoculum of both mutant and WT cells. F, strains resistant to GAM or CIP showed lower MPCs and MICs relative to the WT strain when exposed to antibiotics to which they were collaterally sensitive.

indicated that both CIP^R and GAM^R strains exhibited lower MPCs compared to their WT strain for antibiotics to which they were collaterally sensitive (Fig. 2-F). This collateral sensitivity-based approach to antibiotic therapy can prevent the emergence of resistant mutants at lower concentrations, thereby minimizing the potential for resistance development.

3.3. Increased intracellular accumulation of GAM contributes to collateral sensitivity in CIP-resistant *S. suis*

GAM demonstrated enhanced bactericidal activity against the CIP^R *S. suis* strain compared to the WT. Given that GAM acts in the cytoplasm by binding to the 50S ribosomal subunit, which requires the drug to enter bacterial cells first, we hypothesized that the collateral sensitivity to GAM in the CIP^R *S. suis* strain is due to increased intracellular antibiotic accumulation. To test this hypothesis, we assessed cytoplasmic membrane permeability using NPN, membrane integrity using PI, and membrane potential using $DiSC_3(5)$ in both WT and CIP^R strains. The CIP^R strain consistently showed significantly increased membrane permeability and decreased membrane integrity compared to the WT (P<0.01; Fig. 3-A and B). Membrane disruption in the CIP^R strain resulted in the dissipation of the cytoplasmic membrane potential (Δφ) (P<0.05; Fig. 3-C). WGS analysis of the CIP^R strain revealed a mutation in the *ktrB* gene, which encodes a component of the potassium uptake system (Appendix C). Given the importance of potassium transmembrane transport in maintaining Δφ, the isogenic *ktrB* knockout strain (Δ*ktrB*) exhibited a significant reduction in Δφ compared to its WT parent (P<0.001; Fig. 3-C), mirroring the Δφ dissipation observed in the CIP^R strain.

Δφ is a crucial component of the PMF, which drives essential bacterial processes such as ATP synthesis and efflux pump activity (Yang *et al.* 2023). To investigate this further, we employed the fluorescence probe BCECF-AM and luciferase assays to measure intracellular PMF and ATP levels. Compared to the WT, both the CIP^R and Δ*ktrB* strains exhibited decreased fluorescence intensities, indicating impaired PMF, especially in the presence of CCCP, an uncoupler of oxidative phosphorylation (P<0.05; Fig. 3-D). Similarly, intracellular ATP production was significantly reduced in both the CIP^R and Δ*ktrB* strains compared to the WT, regardless of CCCP presence (P<0.05; Fig. 3-E).

In addition to the *ktrB* mutation, WGS analysis identified a mutation in the *pmrA* gene, which encodes a multidrug resistance efflux pump in the CIP^R strain (Appendix C). Considering the critical role of potassium ion homeostasis in maintaining membrane potential, low expression of *ktrB* in the CIP^R mutant suggests PMF collapse (Fig. 3-F). Since PMF is essential for efflux pump function, we compared *pmrA* expression levels between the CIP^R and WT strains. As expected, *pmrA* expression was lower in the CIP^R strain than in the WT (Fig. 3-G). As a result, we observed significantly increased intracellular GAM accumulation in the CIP^R strain, both in the presence and absence of efflux inhibitors PAβN and CCCP, compared to the WT (Fig. 3-H). Consistently, overexpression of *pmrA* in the WT background [WT(*pmrA*)] led to a significant decrease in intracellular GAM accumulation. Collectively, the disruption of membrane permeability,

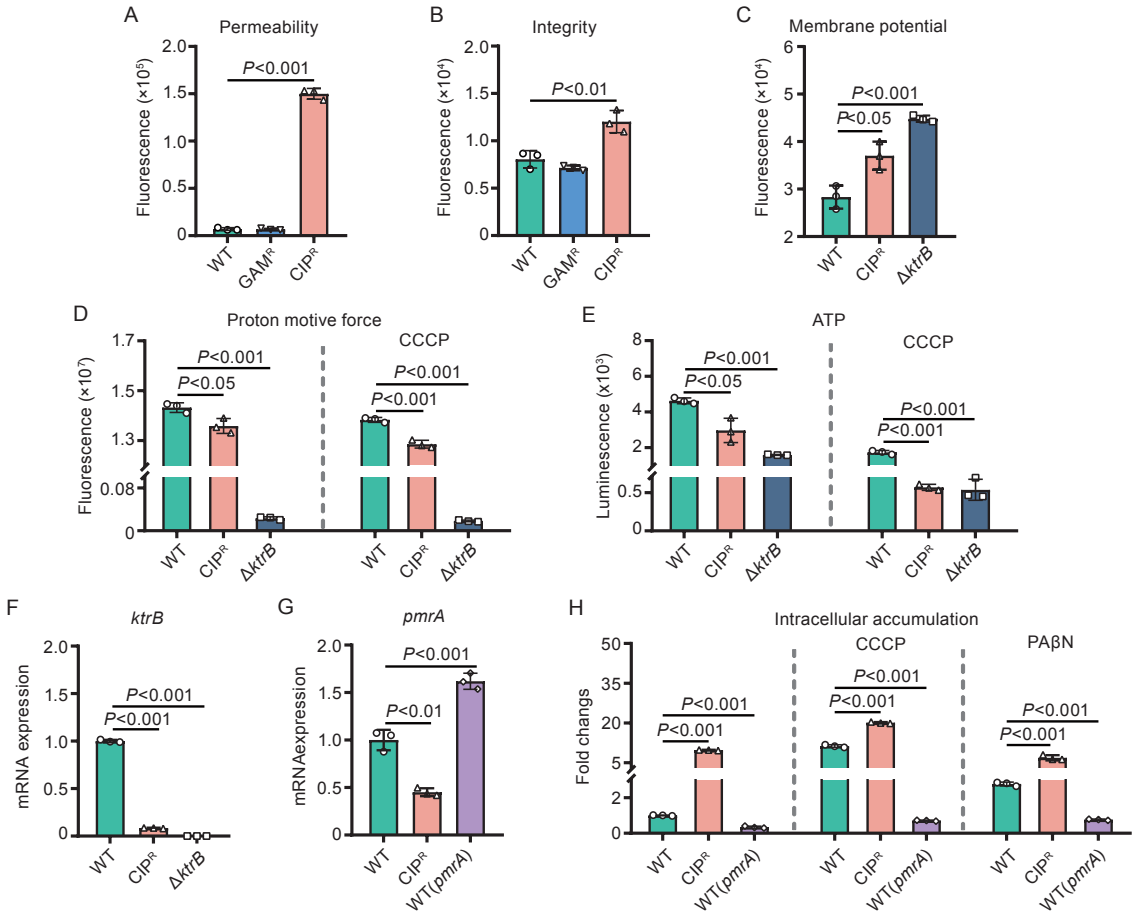


Fig. 3 Increased intracellular accumulation drives collateral sensitivity to gamithromycin in ciprofloxacin-resistant *Streptococcus suis*. A and B, the ciprofloxacin-resistant (CIP^R) *S. suis* mutant exhibits increased plasma membrane permeability and reduced membrane integrity compared to its WT parent, as indicated by NPN (A) and PI (B) fluorescence intensities, respectively. C, the *ktrB* mutation and deletion lead to dissipation of membrane potential in *S. suis* mutants, assessed using the fluorescent dye $DiSC_3(5)$. D, disruption of the proton motive force (PMF) was monitored by measuring fluorescence intensity in bis-carboxyethyl-carboxyfluorescein acetoxymethylester (BCECF-AM)-probed *S. suis* strains, with or without carbonyl cyanide m-chlorophenylhydrazone (CCCP) treatment. E, decreased intracellular ATP production was observed in the CIP^R and Δ*ktrB S. suis* mutants both in the presence and absence of CCCP, measured with a luciferin/luciferase bioluminescence system. F and G, reduced expression levels of *ktrB* (F) and *pmrA* (G) were noted in the CIP^R, Δ*ktrB*, and WT(*pmrA*) strains. H, increased intracellular accumulation of gamithromycin (GAM) in the CIP^R *S. suis* mutant in the presence or absence of PAβN and CCCP. The initial GAM concentration was 2 mg L^{-1}, and intracellular levels were determined using LC-MS/MS analysis. Detailed information about the tested strains, including WT, CIP^R, Δ*ktrB*, and WT(*pmrA*), is provided in Appendix B.

dissipation of transmembrane potential, and inhibition of PMF-driven efflux pump activity result in increased intracellular accumulation of GAM, contributing to the collateral sensitivity of the CIP^R *S. suis* strain to GAM (Fig. 4).

3.4. GAM is an effective treatment against CIP-resistant *S. suis* infections

Next, we tested whether GAM monotherapy can be effective in treating *S. suis* infections due to the CIP^R strain *in vivo* using a murine thigh infection model. We first evaluated the PK properties of GAM in mice after single s.c. doses of 3, 6, and 12 mg kg^{-1} using LC-MS/MS analysis. The plasma PK parameters exhibited a dose-dependent relationship, with both AUC and the maximum concentration (C_{max}) increasing proportionally across the dose range (Fig. 5-A; Appendix D). The long elimination half-life ($T_{1/2\lambda z}$, 13.8–19.1 h; Appendix D) implied that GAM is suitable for once-daily dosing in animals. Given the preferential clearance of the CIP^R strain by GAM *in vitro* based on their collateral sensitivity profiles, we thus used the murine thigh infection model to verify this observation *in vivo*. Following treatment with GAM at 12 mg kg^{-1}, the mean bacterial density in the thighs of mice infected with the CIP^R strain was 3.95 $\log_{10}$cfu g^{-1}, significantly lower than that observed in the WT-infected group (5.16 $\log_{10}$cfu g^{-1}, P<0.05; Fig. 5-B).

To further compare the *in vivo* efficacy of GAM against the CIP^R and WT strains, we established dose-response curves for quantitative analysis (Fig. 5-C). Notably, GAM achieved complete bacterial clearance in CIP^R-infected mice (5.9 $\log_{10}$cfu g^{-1} reduction; Appendix E), whereas a reduction of only 3.35 $\log_{10}$cfu g^{-1} was observed in WT-infected mice, even at the highest dose of 24 mg kg^{-1} (Fig. 5-C). Previous studies have demonstrated that the AUC/MIC surrogate marker is the best predictive PK/PD index for efficacy (Toutain *et al.* 2021). We thus performed PK/PD correlation analysis by quantitatively integrating PK data with *in vivo* efficacy.

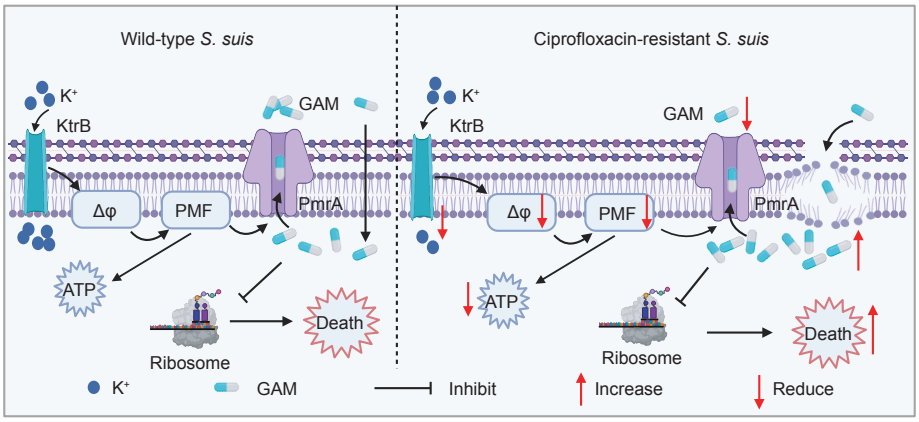


Fig. 4 Mechanistic insight into collateral sensitivity of ciprofloxacin (CIP)-resistant *Streptococcus suis* to gamithromycin (GAM). This figure is created by BioRender (https://BioRender.com) and has confirmed publishing and licensing rights, with agreement number YB27I5KD93. PMF, proton motive force; ATP, adenosine triphosphate.

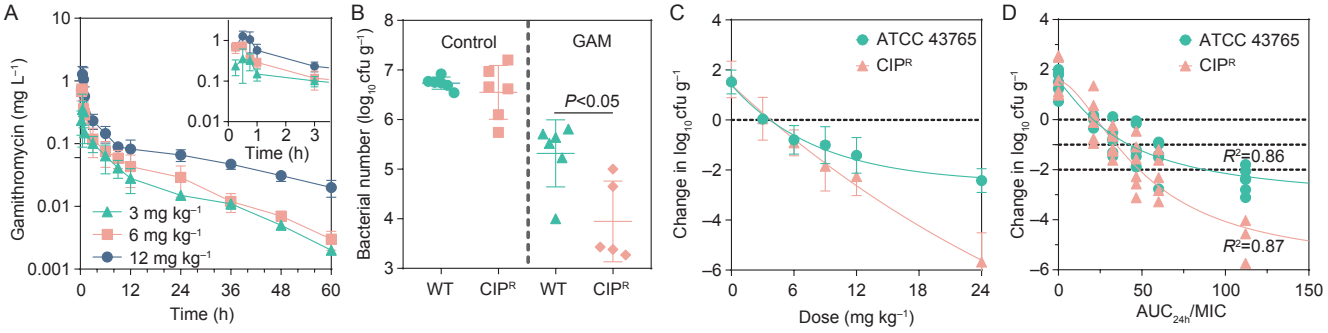


Fig. 5 Collateral sensitivity-based treatments significantly resensitized ciprofloxacin (CIP)-resistant *Streptococcus suis* strains to gamithromycin (GAM) *in vivo*. A, pharmacokinetic profiles of GAM in plasma following subcutaneous administration of single doses of 3, 6, and 12 mg kg^{-1} in mice. The inset shows data plotted from 0 to 3 h. B, bacterial densities of the CIP-resistant *S. suis* mutant and its parental strain in the thighs of mice treated with GAM at 12 mg kg^{-1}. C, *In vivo* dose-response relationship of GAM against the *S. suis* mutant and its parental strain in the murine thigh infection model. Mice received a series of 2-fold increasing GAM doses from 3 to 24 mg kg^{-1}. Each symbol represents the mean $\log_{10}$ change in thigh bacterial burden from five to seven mice (n=5–7 per dose) after 24 h of therapy. Data points below the horizontal dotted line represent bacterial killing, while points above the line represent growth. D, correlations between *in vivo* treatment efficacy of GAM and the PK/PD index of $AUC_{24\,h}$/MIC ratios in plasma against *S. suis* mutant and its parental strain in the murine thigh infection model. The horizontal lines indicate the thresholds for net static, 1-$\log_{10}$, and 2-$\log_{10}$ kill effects, respectively. R^2 represents the coefficient of determination.

The correlations between $AUC_{24\,h}$/MIC and effectiveness were robust, with R^2 of >0.86 for both CIP^R and WT strains (Fig. 5-D). The AUC/MIC targets associated with 1-$\log_{10}$ and 2-$\log_{10}$ kill effects were 35.23 h and 49.95 h, respectively, for the CIP^R strain, compared to 43.71 h and 86.74 h for the WT strain (Appendix E). In particular, the 2-$\log_{10}$ kill $AUC_{24\,h}$/MIC target for the CIP^R strain was only half that of the WT strain.

As GAM is a semisynthetic macrolide antibiotic approved for the treatment of swine bacterial respiratory infections (Yang *et al.* 2019), we next sought to estimate the probability of successfully treating resistant *S. suis* infections in swine with GAM through Monte Carlo simulations. At the current clinical dose of 6 mg kg^{-1}, the PTA for CIP^R infections (100%) was significantly higher than for the WT strain (10.49%; Fig. 6). The calculated GAM doses required to achieve a PTA of >90% were 2.4 and 12.15 mg kg^{-1} for the CIP^R and WT strains, respectively.

4. Discussion

Streptococcus suis is a notable zoonotic pathogen frequently associated with persistent infections in clinical settings, posing a serious threat to human public health and resulting in substantial economic losses in the pig industry (Wertheim *et al.* 2009; Xia *et al.* 2019). Empiric antibiotic therapy remains the primary approach for managing streptococcosis. Data from the United States, Canada, the Netherlands, and Vietnam indicate that *S. suis* is susceptible to penicillin, enrofloxacin, florfenicol, and vancomycin (Mai *et al.* 2008; van Hout *et al.* 2016). However, high resistance rates have been reported for tetracycline (78.4%, MIC_{90}>32 mg L^{-1}) and clindamycin (48.1%, MIC_{90}>8 mg L^{-1}) (van Hout *et al.* 2016). In particular, penicillin resistance has been documented in a single human case and in some pig isolates (Wertheim *et al.* 2009). This underscores the urgent need for effective therapeutic strategies to combat resistant *S. suis* infections. Interestingly, in our study, we observed a robust reciprocal collateral sensitivity between CIP and GAM. Specifically, GAM exhibited markedly enhanced efficacy against CIP-resistant *S. suis* subpopulations. These findings suggest that sequential therapy using the CIP and GAM pair, grounded in

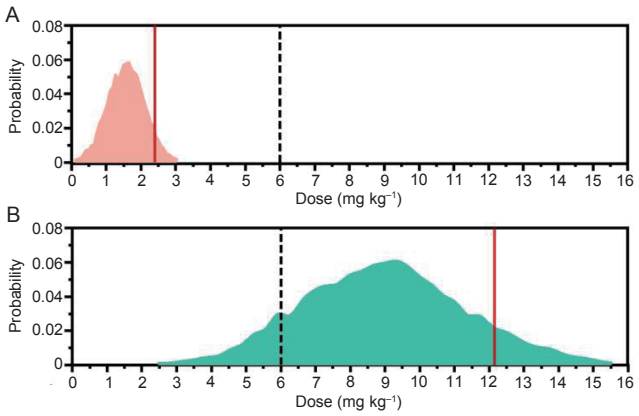


Fig. 6 Gamithromycin (GAM) treatments achieve higher success rates against ciprofloxacin-resistant *Streptococcus suis* mutant (CIP^R) compared to its parental wild-type (WT) strain. A and B, simulated population distributions of GAM dosages in pigs, as predicted by a PK/PD model, for CIP^R (A) and WT (B) strains, expressed in terms of the probability of target attainment (PTA; *y*-axis). The vertical red lines indicate the calculated target dose (2.4 and 12.15 mg kg^{-1}) for a PTA of >90% for treating infections due to the CIP^R *S. suis* mutant and its parental strain, respectively. The vertical black dotted lines indicate the current clinical dose of GAM at 6 mg kg^{-1} in pigs. The distributions on the left represent the PTA for the current dose in effectively treating the CIP^R *S. suis* mutant (100%) and its parental WT strain (10.49%), respectively.

their collateral sensitivity relationship, may offer a promising approach for combating antibiotic-resistant *S. suis* infections.

The prevailing understanding of antibiotic resistance mechanisms relies on the fact that the evolution of resistance is related to drug exposure. Strategic selection of drugs having reciprocal collateral sensitivity profiles may facilitate collateral sensitivity cycling of antibiotics, thereby constraining the evolution of drug resistance in target bacterial populations (Imamovic and Sommer 2013). In this study, a mutation in the *gyrA* gene was found to contribute to the acquisition of quinolone resistance under CIP pressure. However, the development of resistance can be significantly mitigated by antibiotics whose mechanisms of resistance lead to collateral sensitivity. We found that both CIP- and GAM-resistant subpopulations exhibited lower MPCs compared to the WT for the drugs to which they showed collateral sensitivity. Recent findings also suggest that CIP resistance induces collateral sensitivity to aminoglycosides, thereby constraining resistance evolution in *Salmonella typhimurium* (Hasan *et al.* 2023). Additionally, several studies have categorized collateral sensitivity mechanisms into four groups: enhanced drug net uptake, chemical activation, altered cellular response, and increased drug target binding (Roemhild and Andersson 2021). However, the collateral sensitivity mechanism between fluoroquinolones and macrolides in *S. suis* remains poorly understood. Our results attribute the collateral sensitivity relationship to regulatory increases in intracellular antibiotic accumulation, driven by increased penetration of the plasma membrane and reduced antibiotic efflux.

Membrane potential plays an important role in maintaining ion homeostasis and regulating bacterial physiological functions (Ma *et al.* 2023). Disruption in the balance of internal and external ion concentrations can adversely affect bacterial viability (Stautz *et al.* 2021). In particular, the potassium transport system is essential for stabilising membrane potential and ion balance (Stautz *et al.* 2021). In this study, we identified a mutation in the *ktrB* gene of the CIP-resistant *S. suis* strain, which encodes the KtrA/B potassium uptake system. This mutation resulted in significantly reduced *ktrB* expression and decreased K^+ ion uptake, ultimately leading to membrane potential dissipation. Alterations in membrane potential and ion exchange across membranes can increase plasma membrane permeability and drug uptake (Ma *et al.* 2023). Consistent with this, we noted increased membrane permeability and higher intracellular accumulation of GAM in the CIP-resistant *S. suis* strain compared to the WT. This mechanism underlies the collateral sensitivity of CIP-resistant *S. suis* to GAM. Recent studies have also demonstrated that benzydamine and metformin facilitate tetracycline uptake by disrupting membrane potential and pH gradient, thereby reversing antibiotic resistance in multidrug-resistant pathogens (Liu *et al.* 2020; 2021).

In addition to modification by methylation of 23S rRNA and inactivation by phosphotransferases or esterases, major mechanisms of macrolide resistance in Gram-positive bacteria also include upregulation of efflux pumps (Dong *et al.* 2024). The function of these efflux pumps is heavily dependent on the PMF, which consists of membrane electric potential and pH gradient (Yang *et al.* 2023). In the CIP-resistant *S. suis*, increased sensitivity to GAM arises from PMF reduction due to membrane potential dissipation, leading to diminished activity of PMF-dependent multidrug efflux pumps such as PmrA. Additionally, bacterial PMF is crucial for ATP synthesis (Yang *et al.* 2023). We observed lower ATP levels in the CIP-resistant *S. suis*, rendering the efflux pump dysfunctional due to insufficient energy supply. Besides, a single nucleotide polymorphism (SNP) mutation in the *pmrA* gene was found in the CIP-resistant *S. suis*, resulting in reduced mRNA expression compared to the WT strain. These mechanisms, contributing to the loss of membrane potential, PMF energy, and efflux pump function, work together to cause increased intracellular GAM accumulation, resulting in a collateral sensitivity phenotype in CIP-resistant *S. suis*. Similarly, previous studies have demonstrated that increased intracellular accumulation, resulting from weakened efflux pump due to saturated fatty acid-induced PMF reduction, enhances the activity of colistin (Cai *et al.* 2023).

Collateral sensitivity provides a promising avenue for designing treatment strategies to improve therapeutic efficacy and suppress within-host evolution of antibiotic resistance (Roemhild and Andersson 2021). Previous studies have shown that one-directional collateral sensitivity can effectively suppress the emergence of antibiotic resistance (Aulin *et al.* 2021), although our study revealed a reciprocal collateral sensitivity relationship between CIP and GAM. Since one-directional collateral sensitivity relationships are much more common (Imamovic and Sommer 2013), they have the potential to broaden the range of clinical scenarios suitable for effective treatments based on this principle. Thus, one-directional sequential administration is often considered a strategy to

improve antibiotic treatment in the presence of collateral sensitivity. Despite the promising potential of collateral sensitivity-based antibiotic therapy in human clinical cases (Imamovic *et al.* 2018), such approaches remain underexplored in veterinary settings, especially in relation to different classes of veterinary antibiotics and across various animal species. Nevertheless, our research represents an initial effort to apply this approach in veterinary practice, offering new insights and experience for veterinarians combating antibiotic-resistant bacterial infections. In our study, the evolved CIP-resistant *S. suis* strain with collateral sensitivity to GAM demonstrated significantly lower bacterial loads in a murine thigh infection model compared to the WT strain.

Translating *in vitro* findings on collateral sensitivity to *in vivo* or clinical scenarios necessitates consideration of PK/PD correlation, as these factors determine the impacts of different antibiotics on the concentration-dependent effects of bacterial growth, inhibition, and killing (Aulin *et al.* 2021). Our *in vivo* PK/PD analysis revealed that the AUC_{24h}/MIC target of GAM needed to achieve a 2-log_{10} reduction in the CIP-resistant *S. suis* strain was only half of that required for the WT strain. Consequently, the clinical dose of 6 mg kg^{-1} GAM resulted in higher success rates for treating CIP-resistant *S. suis* infections, as indicated by Monte Carlo simulation. This suggests that switching veterinary antibiotics based on collateral sensitivity can provide greater treatment efficacy against multidrug-resistant *S. suis* infections compared to repeated administration of the same antibiotic.

5. Conclusion

In summary, we demonstrated the collateral sensitivity of CIP-resistant *S. suis* to GAM and explored its underlying mechanisms. The increased sensitivity of CIP-resistant *S. suis* mutants to GAM was related to increased intracellular antibiotic accumulation due to the dissipation of bacterial membrane potential and reduced activity of PMF-driven efflux pumps. In addition, our findings from both *in vitro* and murine models indicate that GAM exhibits superior efficacy against CIP-resistant *S. suis* compared to the WT. These results offer valuable insights into potential therapeutic strategies for combating multidrug-resistant *S. suis* infections by exploiting collateral sensitivity-based approaches.

Acknowledgements

This work was supported by the National Key Research and Development Program of China (2023YFD1800100), the National Natural Science Foundation of China (32172909 and 31902318), the Guangdong Basic and Applied Basic Research Foundation, China (2024A1515010365), the Foundation for Innovative Research Groups of National Natural Science Foundation of China (32121004), the Local Innovative and Research Teams Project of Guangdong Pearl River Talents Program, China (2019BT02N054), the Double First-Class Discipline Promotion Project, China (2023B10564003) and the 111 Center, China (D20008). The authors would like to thank BioRender (https://BioRender.com) for their assistance in creating the graphics, as well as Dr. Hao Ren from South China Agricultural University for help with the illustrations.

Declaration of competing interest

The authors declare that they have no conflict of interest.

Declaration of generative AI and AI-assisted technologies in the writing process

The authors declare that they did not use AI in the preparation and writing of this manuscript.

Ethical approval

All mouse experiments were approved by the Institutional Animal Care and Use Committee (IACUC) of South China Agricultural University (approval no. 2022B095 and 2022C014), which were performed in accordance with national and institutional animal welfare and ethics guidelines.

Appendices associated with this paper are available at https://doi.org/10.1016/j.jia.2024.12.005

References

Aulin L B S, Liakopoulos A, van der Graaf P H, Rozen D E, van Hasselt J G C. 2021. Design principles of collateral sensitivity-based dosing strategies. *Nature Communications*, **12**, 5691.

Cai J, Shi J, Chen C, He M, Wang Z, Liu Y. 2023. Structural-activity relationship-inspired the discovery of saturated fatty acids as novel colistin enhancers. *Advanced Science*, **10**, e2302182.

Cao M, Feng Y, Wang C, Zheng F, Li M, Liao H, Mao Y, Pan X, Wang J, Hu D, Hu F, Tang J. 2011. Functional definition of LuxS, an autoinducer-2 (AI-2) synthase and its role in full virulence of *Streptococcus suis* serotype 2. *Journal of Microbiology*, **49**, 1000–1011.

Chen X W, Wu J H, Liu Y L, Munang'andu H M, Peng B. 2023. Fructose promotes ampicillin killing of antibiotic-resistant *Streptococcus agalactiae*. *Virulence*, **14**, 2180938.

CLSI 2020. *Performance Standards for Antimicrobial Disk and Dilution Susceptibility Tests for Bacteria Isolated From Animals: Approved Standard*. 5th ed. Wayne: Clinical and Laboratory Standards Institute (CLSI) Supplement VET01S.

Dong C L, Wu T, Dong Y, Qu Q W, Chen X Y, Li Y H. 2024. Exogenous methionine contributes to reversing the resistance of *Streptococcus suis* to macrolides. *Microbiology Spectrum*, **12**, e0280323.

Dong X, Chao Y, Zhou Y, Zhou R, Zhang W, Fischetti V A, Wang X, Feng Y, Li J. 2021. The global emergence of a novel *Streptococcus suis* clade associated with human infections. *EMBO Molecular Medicine*, **13**, e13810.

Dou Q, Zhu Y, Li C, Bian Z, Song H, Zhang R, Wang Y, Zhang X, Wang Y. 2023. 4F-indole enhances the susceptibility of *Pseudomonas aeruginosa* to aminoglycoside antibiotics. *Microbiology Spectrum*, **11**, e0451922.

Feng Y, Zhang H, Ma Y, Gao G F. 2010. Uncovering newly emerging variants of *Streptococcus suis*, an important zoonotic agent. *Trends in Microbiology*, **18**, 124–131.

Feng Y, Zhang H, Wu Z, Wang S, Cao M, Hu D, Wang C. 2014. *Streptococcus suis* infection. *Virulence*, **5**, 477–497.

Fuentes-Hernandez A, Plucain J, Gori F, Pena-Miller R, Reding C, Jansen G, Schulenburg H, Gudelj I, Beardmore R. 2015. Using a sequential regimen to eliminate bacteria at sublethal antibiotic dosages. *PLoS Biology*, **13**, e1002104.

Gianvecchio C, Lozano N A, Henderson C, Kalhori P, Bullivant A, Valencia A, Su L, Bello G, Wong M, Cook E, Fuller L, Neal III J B, Yeh P J. 2019. Variation in mutant prevention concentrations. *Frontiers in Microbiology*, **10**, 42.

Gonzales P R, Pesesky M W, Bouley R, Ballard A, Biddy B A, Suckow M A, Wolter W R, Schroeder V A, Burnham C A, Mobashery S, Chang M, Dantas G. 2015. Synergistic, collaterally sensitive β-lactam combinations suppress resistance in MRSA. *Nature Chemical Biology*, **11**, 855–861.

Haenni M, Lupo A, Madec J Y. 2018. Antimicrobial resistance in *Streptococcus* spp. *PLoS Biology*, **6**, 10.

Hasan M, Wang J, Ahn J. 2023. Ciprofloxacin and tetracycline resistance

cause collateral sensitivity to aminoglycosides in *Salmonella typhimurium*. *Antibiotics*, **12**, 1335.
Hernando-Amado S, Sanz-García F, Martínez J L. 2020. Rapid and robust evolution of collateral sensitivity in *Pseudomonas aeruginosa* antibiotic-resistant mutants. *Advanced Science*, **6**, eaba5493.
van Hout J, Heuvelink A, Gonggrijp M. 2016. Monitoring of antimicrobial susceptibility of *Streptococcus suis* in the Netherlands, 2013–2015. *Veterinary Microbiology*, **194**, 5–10.
Imamovic L, Ellabaan M M H, Dantas Machado A M, Citterio L, Wulff T, Molin S, Krogh Johansen H, Sommer M O A. 2018. Drug-driven phenotypic convergence supports rational treatment strategies of chronic infections. *Cell*, **172**, 121–134.
Imamovic L, Sommer M O. 2013. Use of collateral sensitivity networks to design drug cycling protocols that avoid resistance development. *Science Translational Medicine*, **5**, 204ra132.
Lázár V, Pal Singh G, Spohn R, Nagy I, Horváth B, Hrtyan M, Busa-Fekete R, Bogos B, Méhi O, Csörgő B, Pósfai G, Fekete G, Szappanos B, Kégl B, Papp B, Pál C. 2013. Bacterial evolution of antibiotic hypersensitivity. *Molecular Systems Biology*, **9**, 700.
Lee W, Hwang J S, Lee D G. 2015. A novel antimicrobial peptide, scolopendin, from Scolopendra subspinipes mutilans and its microbicidal mechanism. *Biochimie*, **118**, 176–184.
Li Q, Chen S, Zhu K, Huang X, Huang Y, Shen Z, Ding S, Gu D, Yang Q, Sun H, Hu F, Wang H, Cai J, Ma B, Zhang R, Shen J. 2022. Collateral sensitivity to pleuromutilins in vancomycin-resistant *Enterococcus faecium*. *Nature Communications*, **13**, 1888.
Liakopoulos A, Aulin L B S, Buffoni M, Fragkiskou E, van Hasselt J G C, Rozen D E. 2022. Allele-specific collateral and fitness effects determine the dynamics of fluoroquinolone resistance evolution. *Proceedings of the National Academy of Sciences of the United States of America*, **119**, e2121768119.
Liu Y, Jia Y, Yang K, Li R, Xiao X, Zhu K, Wang Z. 2020. Metformin restores tetracyclines susceptibility against multidrug resistant bacteria. *Advanced Science*, **7**, 1902227.
Liu Y, Tong Z, Shi J, Jia Y, Deng T, Wang Z. 2021. Reversion of antibiotic resistance in multidrug-resistant pathogens using non-antibiotic pharmaceutical benzydamine. *Communications Biology*, **4**, 1328.
Ma X, Xi W, Yang D, Zhao L, Yu W, He Y, Ni W, Gao Z. 2023. Collateral sensitivity between tetracyclines and aminoglycosides constrains resistance evolution in carbapenem-resistant *Klebsiella pneumoniae*. *Drug Resistance Updates*, **68**, 100961.
Mai N T, Hoa N T, Nga T V, Linh L D, Chau T T, Sinh D X, Phu N H, Chuong L V, Diep T S, Campbell J, Nghia H D, Minh T N, Chau N V, de Jong M D, Chinh N T, Hien T T, Farrar J, Schultsz C. 2008. *Streptococcus suis* meningitis in adults in Vietnam. *Clinical Infectious Diseases*, **46**, 659–667.
Mei J, Jiang X, Li F, Wu Z, Wu T, Zhu J, Jiang H, Li Z, Li N, Lei L. 2025. *Streptococcus suis* serotype 2 collagenase-like protease promotes meningitis by increasing blood–brain barrier permeability. *Journal of Integrative Agriculture*, **24**, 4379–4394.
Pan Z, He P, Zhang Y, Gu Q, Chen S, Yu Y, Shao J, Wang K, Wu Z, Yao H, Ma J. 2022. SssP1, a Fimbria-like component of *Streptococcus suis*, binds to the vimentin of host cells and contributes to bacterial meningitis. *PLoS Pathogens*, **18**, e1010710.
Qu Q, Cui W, Huang X, Zhu Z, Dong Y, Yuan Z, Dong C, Zheng Y, Chen X, Yuan S, Li Y. 2023. Gallic acid restores the sulfonamide sensitivity of multidrug-resistant *Streptococcus suis via* polypharmaceology mechanism. *Journal of Agricultural and Food Chemistry*, **71**, 6894–6907.
Roemhild R, Andersson D I. 2021. Mechanisms and therapeutic potential of collateral sensitivity to antibiotics. *PLoS Pathogens*, **17**, e1009172.
Roemhild R, Linkevicius M, Andersson D I. 2020. Molecular mechanisms of collateral sensitivity to the antibiotic nitrofurantoin. *PLoS Biology*, **18**, e3000612.
Segura M. 2009. *Streptococcus suis*: An emerging human threat. *Journal of Infectious Diseases*, **199**, 4–6.
Segura M. 2015. *Streptococcus suis* vaccines: Candidate antigens and progress. *Expert Review of Vaccines*, **14**, 1587–1608.
Shi K, Li Y, Xu M, Zhang K, Gou H, Li C, Zhai S. 2024. Membrane vesicles derived from *Streptococcus suis* serotype 2 induce cell pyroptosis in endothelial cells via the NLRP3/Caspase-1/GSDMD pathway. *Journal of Integrative Agriculture*, **23**, 1338–1353.
Stautz J, Hellmich Y, Fuss M F, Silberberg J M, Devlin J R, Stockbridge R B, Hänelt I. 2021. Molecular mechanisms for bacterial potassium homeostasis. *Journal of Molecular Biology*, **433**, 166968.
Szybalski W, Bryson V. 1952. Genetic studies on microbial cross resistance to toxic agents. I. Cross resistance of *Escherichia coli* to fifteen antibiotics. *Journal of Bacteriology*, **64**, 489–499.
Tang J, Wang C, Feng Y, Yang W, Song H, Chen Z, Yu H, Pan X, Zhou X, Wang H, Wu B, Wang H, Zhao H, Lin Y, Yue J, Wu Z, He X, Gao F, Khan A H, Wang J, *et al.* 2006. Streptococcal toxic shock syndrome caused by *Streptococcus suis* serotype 2. *PLoS Medicine*, **3**, e151.
Toutain P L, Pelligand L, Lees P, Bousquet-Mélou A, Ferran A A, Turnidge J D. 2021. The pharmacokinetic/pharmacodynamic paradigm for antimicrobial drugs in veterinary medicine: Recent advances and critical appraisal. *Journal of Veterinary Pharmacology and Therapeutics*, **44**, 172–200.
Wang C Z, Wang M G, Chu Y F, Sun R Y, Li J G, Li X A, Sun J, Liu Y H, Zhou Y F, Liao X P. 2023. Antibiotic resistance patterns and molecular characterization of *Streptococcus suis* Isolates from swine and humans in China. *Microbiology Spectrum*, **11**, e0030923.
Wang R L, Liu P, Chen X F, Yao X, Liao X P, Liu Y H, Sun J, Zhou Y F. 2022. Pharmacodynamic target assessment and PK/PD cutoff determination for gamithromycin against *Streptococcus suis* in piglets. *Frontiers in Veterinary Science*, **9**, 945632.
Wei X Y, Zhang J, Zhang Y, Fu W Z, Zhong L G, Pan Y D, Sun J, Liao X P, Liu Y H, Zhou Y F. 2024. Pharmacokinetic/pharmacodynamic evaluation of gamithromycin against rabbit pasteurellosis. *BMC Veterinary Research*, **20**, 147.
Weng Z, Zeng F, Wang M, Guo S, Tang Z, Itagaki K, Lin Y, Shen X, Cao Y, Duan J A, Wang F. 2023. Antimicrobial activities of lavandulylated flavonoids in *Sophora flavences* against methicillin-resistant *Staphylococcus aureus* via membrane disruption. *Journal of Advanced Research*, **57**, 197–212.
Wertheim H F, Nghia H D, Taylor W, Schultsz C. 2009. *Streptococcus suis*: An emerging human pathogen. *Clinical Infectious Diseases*, **48**, 617–625.
Wyns H, Meyer E, Plessers E, Watteyn A, De Baere S, De Backer P, Croubels S. 2014. Pharmacokinetics of gamithromycin after intravenous and subcutaneous administration in pigs. *Research in Veterinary Science*, **96**, 160–163.
Xia X, Qin W, Zhu H, Wang X, Jiang J, Hu J. 2019. How *Streptococcus suis* serotype 2 attempts to avoid attack by host immune defenses. *Journal of Microbiology*, *Immunology*, *and Infection*. **52**, 516–525.
Yang B, Tong Z, Shi J, Wang Z, Liu Y. 2023. Bacterial proton motive force as an unprecedented target to control antimicrobial resistance. *Medicinal Research Reviews*, **43**, 1068–1090.
Yang Q, Liu X, Zhang C, Yong K, Clifton A C, Ding H, Liu Y. 2019. Pharmacokinetics and pharmacodynamics of gamithromycin treatment of *Pasteurella multocida* in a murine lung infection model. *Frontiers in Pharmacology*, **10**, 1090.
Yoshida M, Reyes S G, Tsuda S, Horinouchi T, Furusawa C, Cronin L. 2017. Time-programmable drug dosing allows the manipulation, suppression and reversal of antibiotic drug resistance *in vitro*. *Nature Communications*, **8**, 15589.
Yu H, Jing H, Chen Z, Zheng H, Zhu X, Wang H, Wang S, Liu L, Zu R, Luo L, Xiang N, Liu H, Liu X, Shu Y, Lee S S, Chuang S K, Wang Y, Xu J, Yang W. 2006. Human *Streptococcus suis* outbreak, Sichuan, China. *Emerging Infectious Diseases*, **12**, 914–920.
Zhao Z, Wen S, Song N, Wang L, Zhou Y, Deng X, Wu C, Zhang G, Chen J, Tian G B, Liang M, Zhong L L. 2023. Arginine-enhanced antimicrobial activity of nanozymes against gram-negative bacteria. *Advanced Healthcare Materials*, **13**, e2301332.
Zheng C, Wei M, Jia M, Cao M. 2020. Involvement of various enzymes in the physiology and pathogenesis of *Streptococcus suis*. *Veterinary Sciences*, **7**, 143.
Zhou Y F, Bu M X, Liu P, Sun J, Liu Y H, Liao X P. 2020. Epidemiological and PK/PD cutoff values determination and PK/PD-based dose assessment of gamithromycin against *Haemophilus parasuis* in piglets. *BMC Veterinary Research*, **16**, 81.

Executive Editor-in-Chief Dongming Zhao
Managing Editor Yanyan Sun